STRUCTURE OF A STEADY-STATE COLD LOW

TOBY N. CARLSON

National Hurricane Research Laboratory, ESSA, Miami, Fla.

ABSTRACT

Analyses drawn from the synoptic data gathered over the eastern Caribbean in Project ECCRO, October 1965, revealed the presence of an upper tropospheric cold Low. (With assumption of state motion), the fields of wind, height, temperature, water vapor, vertical velocity, clouds, and weather were transferred to a relative coordinate system traveling with the motion of the cold Low. This process yielded composite fields in which the 6 days of data were combined into 1. These fields, showing the structure of the cold Low at five different levels in the troposphere, are presented and the evolution of cloud and moisture patterns are discussed.

1. INTRODUCTION

During the middle of October 1965, an upper tropospheric cold core cyclone, the so-called "cold Low," moved westward over the Antilles and across the eastern Caribbean. At the same time an intensive reconnaissance expedition, known as Project ECCRO (Eastern Caribbean Cooperative Reconnaissance Operation), was engaged in gathering meteorological data in this area for research purposes by means of simultaneous multi-level aircraft flights and special radiosonde ascents. Although the primary purpose of the project was to determine the variability of the data in the Tropics and the ability of the measurements to resolve this variability during a characteristic period, the analyses also afforded a rather detailed description of about two-thirds of the cold Low's circulation. The purpose of this paper is to show the distribution of height, wind, temperature, water vapor, and cloud cover around the cold Low to the full extent permitted by the ECCRO coverage.

The cold Low is one of the most common features of the weather map at low latitudes during the summer. It has become subject to increasing investigation of late with the advent of good quality satellite photographs and intensified research into the causes of hurricane formation. Research carried out by Simpson [11], Riehl [9], Ricks [8], Rosenthal [10], Frank [3], [4], and Krishnamurti and Baumhefner [5] has formed a concept of the typical cold Low which can be summarized as follows: cold Low are known to exist alone or in chains of vortices and are found over both the Atlantic and Pacific Oceans. Those in the Atlantic tend to originate near the Azores and travel steadily westward near lat. 20°N. They are thought to originate in higher latitudes following the southward extension of the middle Atlantic trough. Typically the system extends about 1,200 mi. from north to south and 2,500 mi. east to west. Many of these systems are not detectable in the low-level winds but are often revealed in the low-level temperature field as a cold trough in the easterlies which increases in intensity with height. The lowest level of closed circulation is commonly between 700 and 500 mb. but occasionally the vortex extends well below 700 mb. The maximum temperature variation between the center of the cold Low and its periphery is found near 300 mb., and the maximum height gradient and wind speed occur near 200 mb., the level where the temperature gradient becomes reversed from that below. Winds are light in the lower-middle troposphere, but the wind speed increases with height and at high levels the strongest winds are found some distance west and northwest of the center. The center of the closed circulation tends to slope with height toward the coldest air which lies northeast of the vortex.

The most notable rainfall and convection occur a few hundred miles from the center, usually in the southeast quadrant. Squalls and thunderstorms are often confined to a relatively narrow belt embedded within a much larger cloud cover over the eastern semicircle. Most of this cloud consists of altocumulus and cirrus beneath which the lower cloud forms tend to be suppressed or absent. There is considerable variation in cloud cover and distribution from one disturbance to another. Some systems have been known to be cloud free for a time. The vertical motion pattern is not symmetric but resembles a dipole with centers of rising and sinking motion east and west of the vortex, respectively. Strongest upward motions are naturally associated with the areas of intense convection but both ascending and descending motions are inherent in the baroclinic nature of the system.

The disturbance may either weaken or intensify. In the former instance the decrease in strength is thought to be due to an insufficient source of kinetic energy, while intensification may be promoted by a direct conversion of potential to kinetic energy through release of latent heat along the periphery. On the other hand an increase in the intensity of convection, possibly occurring near the center, may lead to the formation of a warm core easterly wave or vortex and a disintegration of the cold Low.

2. DATA AND ANALYSIS

The ECCRO aircraft flights were made at five different levels on each of the 6 days of the project: October 12–14 and 16–18, 1965.[1] The planes, belonging to the Weather Bureau Research Flight Facility (RFF), Air Force, and Navy squadrons, were assigned to fly close to the standard levels of 1000, 850, 700, 500, and 250 mb. (The actual levels flown were 976, 841, 691, 501, and 238 mb.) The plan was to start from Puerto Rico, proceed counterclockwise along the path shown in figure 1, and return to the point of departure after a time interval centered on 1800 GMT and lasting from 5 to 12 hr. All aircraft were equipped to measure wind, pressure, altitude, and temperature. The RFF flights were carried out at 700 and 850 mb. on most days, but on two occasions, the 14th and 16th, they were made at 700 and 500 mb. The remainder of the 500-mb. missions and those flown at 250 mb. were carried out by the Air Force. Naval aircraft flew the lowest levels and both the Navy and RFF planes were equipped also to measure water vapor. Thus, humidity was determined on 2 days at 500 mb.

Observations were recorded on data log sheets at intervals of about 15 min. On the RFF flights the information was also recorded digitally at 10-sec. intervals on magnetic tape. Some of the missions made provisions for observing and recording detailed accounts of cloud and weather. Also available as an aid in the reconstruction of cloud and weather patterns were photographic records taken from nose- and side-mounted motion picture cameras and a vertical scan radar on both the RFF aircraft.

The special radiosonde ascents were made at 1800 GMT at San Juan, Santo Domingo, St. Martin, and Curacao (for the location of these stations see fig. 1). Regularly scheduled transmissions of soundings were received from Antigua, Guadeloupe, Chaguaramas (Trinidad), and Barbados, and a few pibals from Lamintin, Roosevelt Roads, Gustavia, and Maracay. Also received were numerous surface reports from the land stations around the border of figure 1, and from a few ships in the interior.

A detailed discussion of data reduction techniques, data accuracy, and analysis procedures will not be presented here, because these topics have been covered previously by the author [2]. The basic data fields are those of wind (streamlines and isotachs), temperature, mixing ratio, geopotential height, and vertical velocity. Only the last two fields refer to the standard isobaric surfaces, rather than actual flight levels. The numerical values were transferred to punch cards in the form of a grid array of 10×13 points and spacing 1° longitude (108 km.) on the original base maps. The weather patterns were reconstructed from the observations in the form of simplified whole sky maps whose various letter designations delineate regions having more or less the same type of cloud distribution. These groupings also correspond closely to the numerical categories in the Tropical Whole Sky Code of Malkus and Riehl [7].[2]

The sequence of anlayses showed that an upper tropospheric cold-core system moved steadily westward during thr 6-day period at a speed of about 2½ kt. Between the 12th and the 14th the weather over the whole area shown in figure 1 was characterized by a widespread suppression of cloud forms and a lack of precipitation. On the 15th the vortex center crossed the Lesser Antilles at about lat. 17°–18°N. The westward movement of the system was accompanied by a corresponding shift westward in the vertical motion and weather patterns so that disturbed weather conditions appeared west of the Antilles after the 15th. However, there was a gradual weakening of the circulation and a warming of the cold core after the 14th. Whereas the vortex had extended down to the 850–700-mb. layer until the 14th, the lowest level of closed circulation after the 14th or 15th was between 700 and 500 mb. Between the 17th and 18th a marked decrease in the amount of convection and a disorganization of the cloud pattern occurred east of the upper trough. At the same time the cumulus in the previously suppressed area west of the trough became much more active.

3. THE COMPOSITE LOW

Despite the diminution in intensity of the system over the whole period, the cold Low seemed to have been in a reasonably steady state, because the changes in temperature and thickness at the center of the cold Low were small compared to the total gradients. These changes amounted to less than 1° C. in temperature at 501 mb. and 30 m. in the 250–500-mb. thickness over the 6 days. The assumption of steady state motion permitted the

[1] No mission was flown at 500 mb. on the 13th.

[2] Thus the area designated by the letter A (not appearing in the composite) corresponds to category 0 in the Tropical Sky Code, B to 1, C to 3, D to 6, E to 8, G to 16, H to 13, and I to 11 or 12. The high cloud symbols X or Y correspond to categories 7, 5, 9, or 10 when used in connection with B, C, D, or E, respectively.

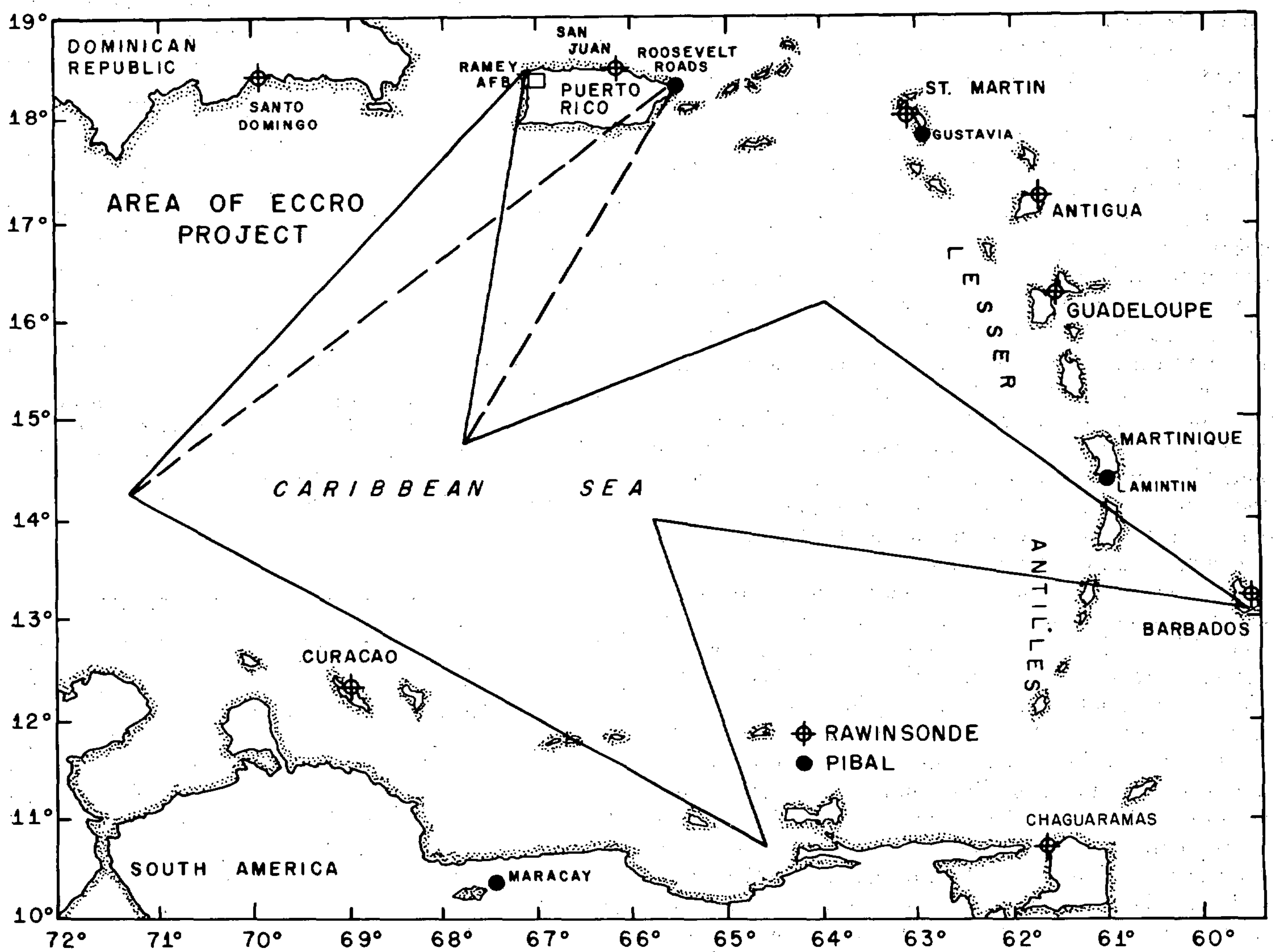

FIGURE 1.—Map showing area of Project ECCRO. The flight path is indicated by connected line segments (shown dashed for track of RFF and Navy planes).

adoption of a moving coordinate system within which the data from all 6 days were composited to yield a time-averaged analysis of each of the numerical fields. Composite fields were constructed from the ECCRO analyses by displacing the numerical fields longitudinally by one grid length (2½ kt. times 24 hr.) per day, averaging the values at each grid point according to the number of overlapping values at that point, and smoothing around the western and eastern boundaries where only one or two points were used to determine a composite value. The result of the compositing was to generate a new 10×19 grid field covering a greater area than any of the individual maps. The grid rows and columns still corresponded, respectively, to latitude and longitude, except that the longitude has no geographical significance. Perhaps the only important inconsistency introduced by the method was some lack of correspondence between the wind and height fields due to the differing ways in which a vector and scalar field are averaged and also to the fact that the wind vectors used in constructing the streamlines and isotachs had the motion of the cold Low subtracted from them.

The streamlines and isotachs for the five levels are presented in figures 2–6 and the geopotential height and thickness contours in figures 7–11. The latter field was constructed primarily with the aid of reported station heights and the observed wind field, and guided somewhat by the aircraft D-values which proved to be of secondary value. The disturbance is faintly visible on these maps at the lowest levels but the cyclonic circulation is not strikingly apparent except at 700 mb. and above. In both fields the axis of the trough appears to slope toward the east above 700 mb.; at 250 mb. the vortex lies about 150 mi. northeast of the 500-mb. center. The temperature analyses in figures 12–16 show a trough of cold air at lower levels in association with the upper vortex. At 500 mb. the center of cold air is east of the cold trough at 700 mb. Judging from the thickness pattern (figs. 10 and 11) the cold core appears vertically aligned between 500 and 250 mb., and is centered just to the northeast of the 250-mb. vortex. Notably higher amounts of moisture (see also figs. 12–16) are visible over the eastern part of the cold Low at all levels except 1000 mb. On that surface the moisture distribution is reversed from the one above. Whereas the largest values of mixing ratio aloft generally are located in the southeast quadrant south of 15° lat., a zone of drier air is found there at 1000 mb. This is thought to be due to the effect of relatively localized areas of lower moisture values, which possibly resulted from outflow produced by cumulonimbi downdrafts, being impressed upon the large-scale pattern in the composite by the longitudinal displacement and averaging of the individual data.

A composite cloud and weather pattern was constructed following a procedure used in handling the numerical fields. The daily patterns, referred to in the previous section, were displaced graphically to set them in the relative coordinate system. Each grid point was then examined with respect to the various code symbols delegated to that point and a representative one chosen to appear in the composite. This composite weather pattern is shown in figure 17. The symbols G, H, and I together represent the total significant cloud cover associated with the cold Low. The region of significant convection (stippled area, I) is shown to occupy only a small fraction of the total cloud cover. This convection was located near the southern portion of the cloud shield and well to the southeast of the 500-mb. vortex center. To the west of the 500-mb. trough the cloud forms were mainly fair weather trade cumulus types (areas B, C, and D). The cloud cover corresponds closely to the distribution of moisture aloft (figs. 13–16); highest values of moisture are found not far from the region of convection.

The cloud shield, visible as a compact and bright cloud area in the TIROS satellite photograph for the 17th (fig. 18), was beginning to disintegrate on the 18th (fig. 19). However, as on the other days, the cloud cover extended some distance north of lat. 19° and was decidedly east of the upper trough at all latitudes.

Before proceeding to the composite vertical velocities it is necessary to describe the manner in which they were computed for the individual daily maps. Because value of divergence that are computed kinematically from the reported winds contain a very high percentage of error, a routine integration of the continuity equation usually results in unsatisfactory patterns of vertical motion. An unfortunate characteristic of kinematical vertical motions

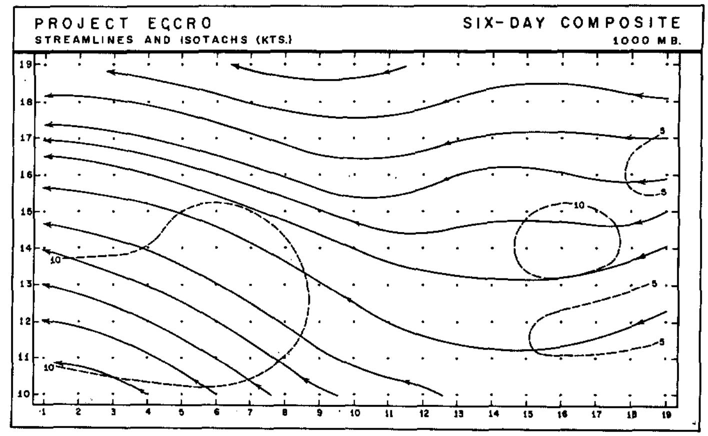

FIGURE 2.—Composited streamlines (solid barbed lines) and isotachs (dashed and labelled in knots) relative to motion of cold Low for 1000 (976) mb., October 12–18, 1965. Grid rows are labelled in degrees of latitude. Columns 1 through 19 are equivalent to parallels at longitude with west on the left.

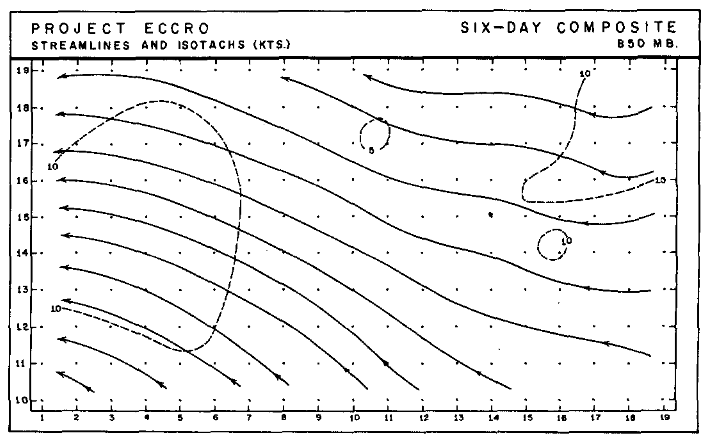

FIGURE 3.—Same as figure 2 but for 850 (841) mb.

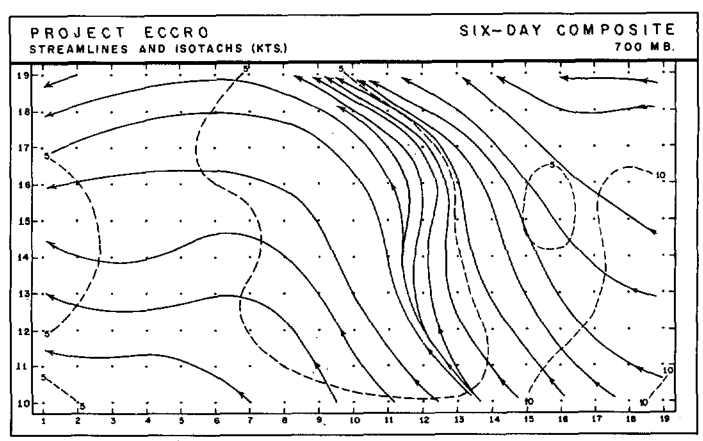

FIGURE 4.—Same as figure 2 but for 700 (691) mb.

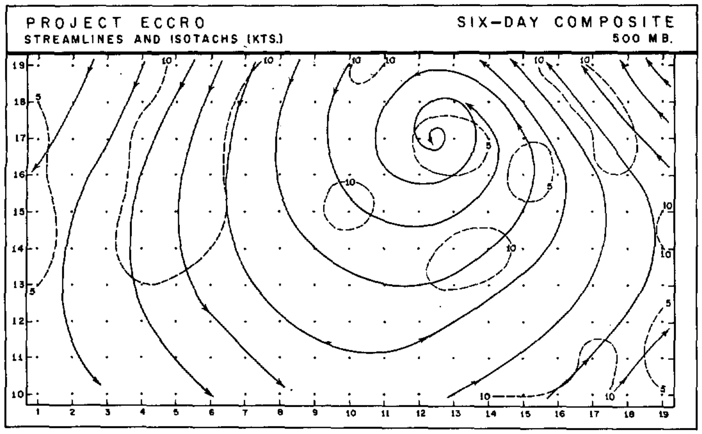

FIGURE 5.—Same as figure 2 but for 500 (501) mb.

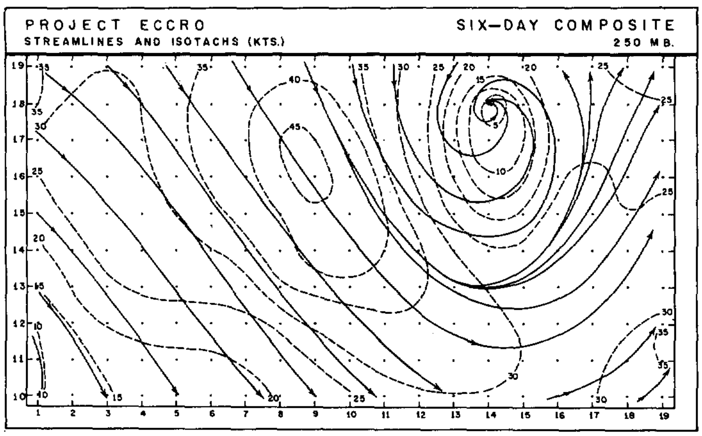

FIGURE 6.—Same as figure 2 but for 250 (238) mb.

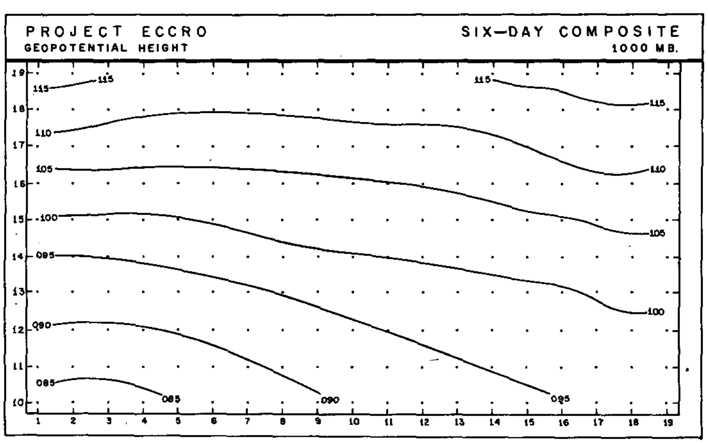

FIGURE 7.—Composited contours of geopotential height at 1000 mb. labelled at 5-m. intervals, October 12–18, 1965.

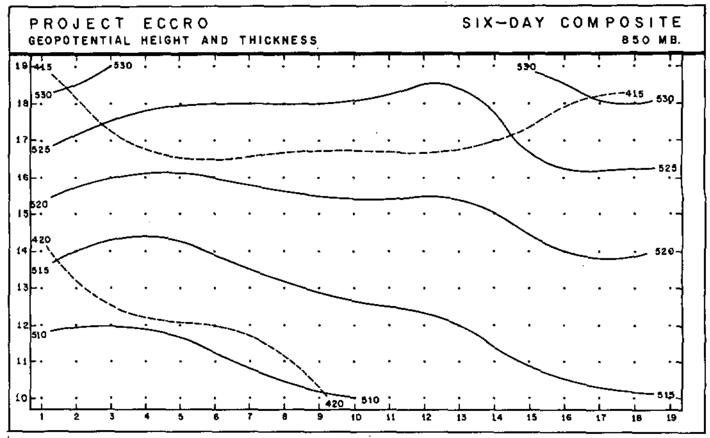

FIGURE 8.—Composited contours of geopotential height (solid lines) at 850 mb. labelled at 5-m. intervals, October 12–18, 1965. Thickness contours (dashed lines) refer to 850–1000-mb. layer. Thousands digit omitted from values of heights and thicknesses.

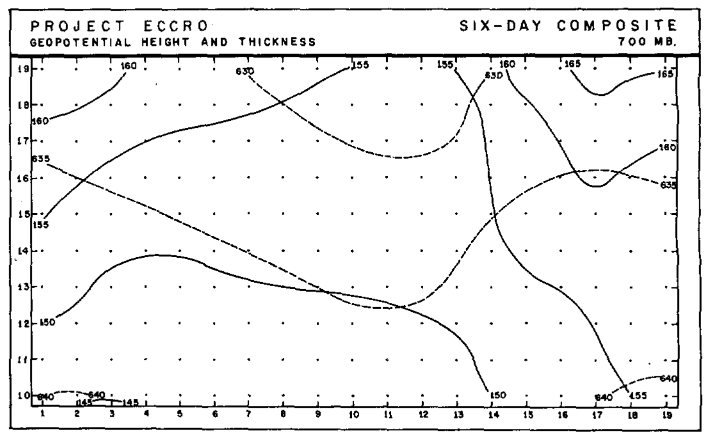

FIGURE 9.—Same as figure 7 but for 700 mb. Dashed thickness lines refer to 700–850-mb. layer.

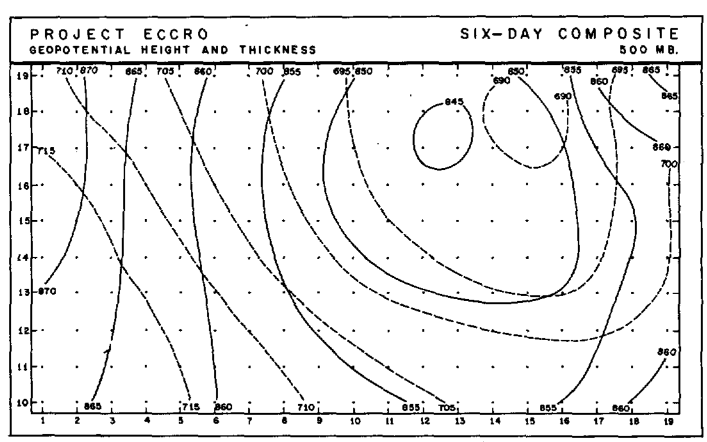

FIGURE 10.—Same as figure 7 but for 500 mb. Dashed thickness lines refer to 500–700-mb. layer.

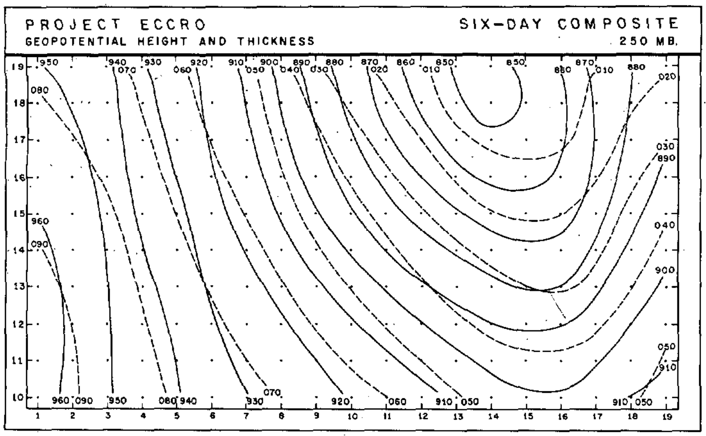

FIGURE 11.—Same as figure 7 but for 250 mb. Dashed thickness lines refer to 250–500-mb. layer. Contours labelled at 10-m. intervals with ten thousands and thousands digits omitted from height values.

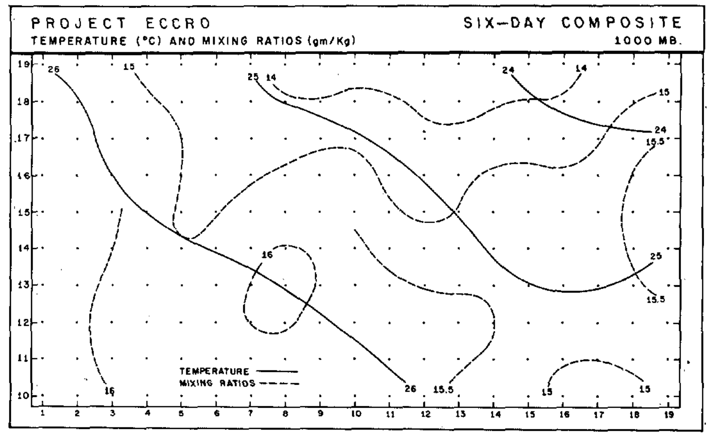

FIGURE 12.—Composited distribution of temperature (solid lines labelled in ° C.) and mixing ratios (dashed lines labelled in gm./kgm.) at 1000 (976) mb., October 12–18, 1965.

is not only the unreasonably large magnitude at the centers of ascending and descending motions but the tendency for the values to increase with height indefinitely. An attempt to minimize the uncertainty in kinematic vertical velocity patterns was made using a slightly different technique from that based on a simple integration of the continuity equation. The mean divergence in the column from 1000 to 100 mb. was constrained to vanish by use of a numerical scheme whereby the vertical motion was adjusted to be zero at the bottom and top of the column and the excess divergence converted to a pressure-averaged constant and subtracted from the initial divergence value at each level (see Lateef [6] and Carlson [2]). The "vertically-balanced" vertical velocity, ω, was obtained by solving a pressure-differentiated form of the continuity equation $(\partial/\partial p)\ (\nabla\cdot\mathbf{V})=\partial^2\omega/\partial p^2$, where $\nabla\cdot\mathbf{V}$ is the horizontal velocity divergence. Since the divergence was not determined at 100 mb. a further constraint was applied to the solution of the above equation. It was assumed that the vertical velocity at 250 mb. could be approximated by the expression for isentropic steady state motion $-(\mathbf{V}-\mathbf{C})\cdot\nabla\theta/S$, where θ is the potential temperature on the 250-mb. surface and $S(=\partial\theta/\partial p)$ is the lapse rate. The system's velocity of translation, $\mathbf{C}$, was taken as one degree of latitude per day toward the west.

A finite differencing method for solving the equation was used to determine "quasi-kinematic" vertical velocities. These are presented for the levels 850, 700, and 500 mb. in figures 20–22. For comparison with the quasi-kinematic ones, the vertical velocities at the corresponding levels were computed solely from the formula for isentropic steady-state motion and are presented in figures 23–25. The (adiabatic) vertical velocity distribution at 250 mb.,

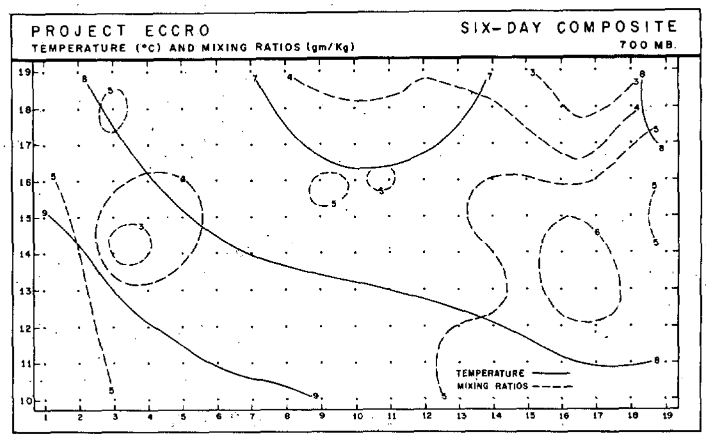

FIGURE 13.—Same as figure 12 but for 850 (841) mb.

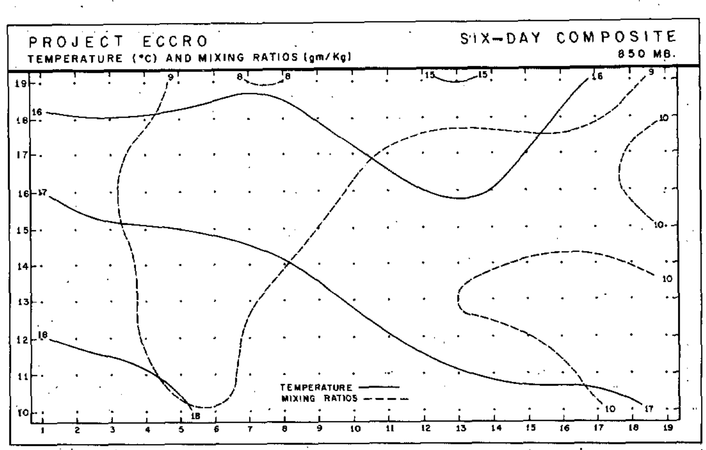

FIGURE 14.—Same as figure 12 but for 700 (691) mb.

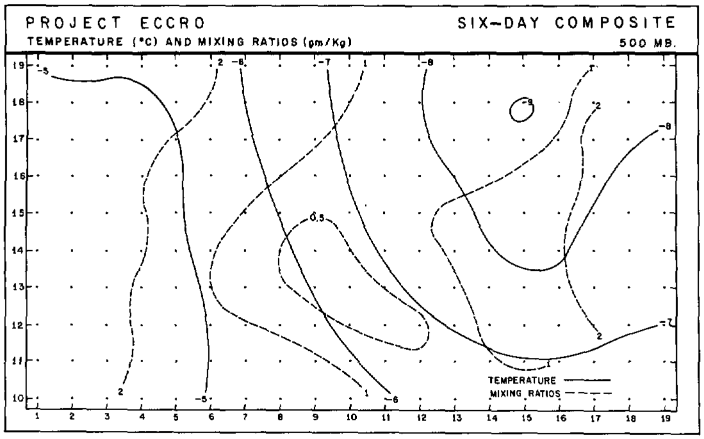

FIGURE 15.—Same as figure 12 but for 500 (501) mb. Composited mixing ratios based on only 2 days of data.

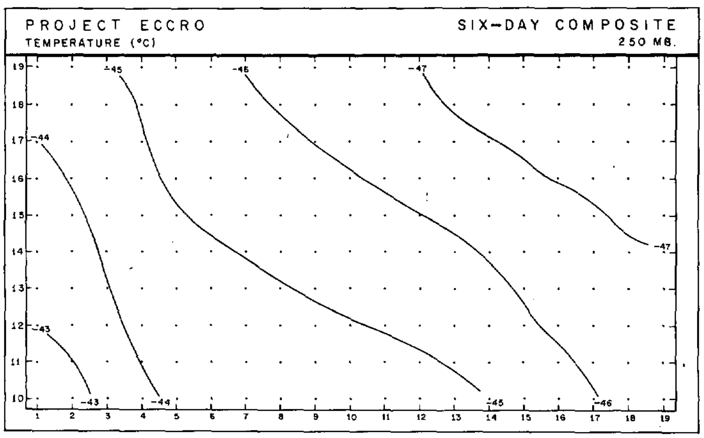

FIGURE 16.—Composited distribution of temperature (in ° C.) for 250 (238) mb., October 12–18, 1965.

common to both sets of vertical motion maps, is shown in figure 26. For the central values of ascending and descending flows, the adiabatic vertical motions are generally about half an order of magnitude smaller than the quasi-kinematic ones, but the two representations of the same field bear some resemblance to each other insofar as both patterns show a wide area of descent on the western side of the upper trough, approximately coinciding with the region of dry fair weather, and a region of ascent east of the upper trough in the area of cloudiness and precipitation. At the center of the vortex the vertical motion was nearly zero, with slight descent predominating. Near the western edge of the grid some ascent is shown at low levels in the kinematic patterns. The patterns of quasi-kinematic vertical velocity appear rather unsatisfactory at lower levels (figs. 20 and 21) east of the upper trough. There, ascending motion is shown to cover a rather limited area near the southwestern edge of the cloud shield, while descending motion is both stronger and more extensive than ascent and covers much of the region of convection. The magnitude of the quasi-kinematic vertical motion is thought also to be too large. While the adiabatic formula undoubtedly underestimates the actual strength of the vertical motions in the presence of condensation, the only significant non-adiabatic effect at middle levels in the cloud-free region immediately west of the upper trough was the long wave radiation cooling. Assuming the contribution by radiation to the downward vertical motion to be 0.3 cm./sec. in clear air (equivalent to a radiational cooling of 1.5° C./day), the maximum possible descent at middle levels west of the trough would have been no larger than 0.6–0.8 cm./sec. (see fig. 25), as compared with more than 2 cm./sec. given by the quasi-kinematic method (see fig. 22).

4. DISCUSSION OF DISTRIBUTION OF CLOUD, MOISTURE, AND VERTICAL MOTION AROUND THE COLD LOW

In a previous investigation, Frank [3] observed that only a small fraction of the total cloud cover associated with a particular cold Low contained a significant amount of convection, while the remainder of the overcast consisted of layers of middle and upper cloud beneath which the convection was highly suppressed. The same kind of cloud distribution was found here. The significant convection covered a relatively small area a few hundred miles southeast of the vortex. Examination of the synoptic records revealed that a dense cover of middle cloud (mostly altocumulus) and high cloud (cirrostratus) persisted for 3 or 4 days over the Antilles, but the only stations experiencing appreciable rainfall were situated in the southern part of the chain between Guadeloupe and Trinidad in South America. Amounts up to an inch were recorded near Lamintin, but even there the rainfall was accumulated during the course of about 1 day. North of Guadeloupe the passage of the cold Low brought only scattered showers.

An interesting aspect of the cloud pattern, not apparent in the composite, was the sharply defined edge between the convective region and the fair weather to the west. When approaching the cloud shield from the west by aircraft it was observed that the fair weather extended to the edge of the convection which, on the 16th and 17th, was marked by a wall of cumulonimbi rising to great heights. As the aircraft began to penetrate the cloud the environment became obscured and chaotic, the only recognizable cloud forms being convective towers. Somewhat farther into the cloud system, breaks in the overcast appeared revealing extensive banks and rows of cumulonimbi and clouds of lesser convective development. Radar and

278-472 O - 67 - 5

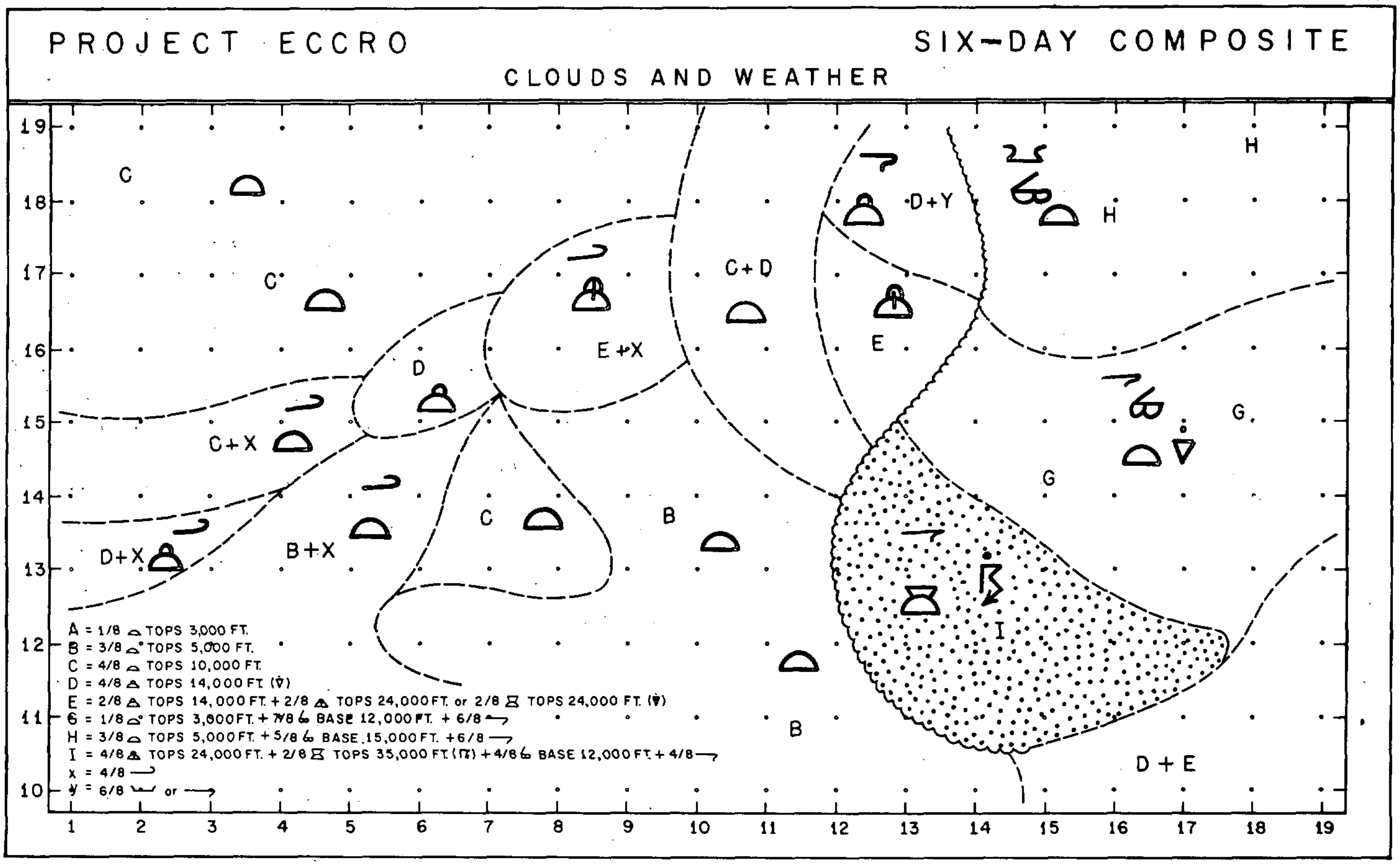

FIGURE 17.—Composited whole sky code map for October 12–18, 1965. Scalloped bordering delineates edge of main cloud shield. Dashed lines signify an indistinct or gradual transition of cloud type between partitioned areas. Shading denotes region of significant convection.

visual observations revealed that many of these cloud banks were merging with a cloud cover containing a low degree of convective activity. Still farther toward the east the cloud cover tended to change to a dense canopy of altocumulus and altostratus which, in places, stretched unbroken to the horizon. Through occasional breaks in the cloud large amounts of cirrus could be seen. Although the layer cloud was of considerable depth it was not totally visible on the airborne vertical scan radar. It was common, however, to observe one or more horizontal bands of precipitation echo at various altitudes. Often such a band was located near the freezing level at 16,000 ft. (the so-called bright band) and occasionally it was broken into a series of generating cells. Beneath the middle cloud base (11,000 ft. near lat. 14°N. and somewhat higher farther north) were only scattered cumulus and patches of stratocumulus, interrupted by occasional showers falling from the middle cloud deck.

Figure 27 shows the flow pattern relative to the motion of the cold Low on the isentropic surface $\theta=39.5°$ C. ($\sim$313° A.). Constructed by interpolation between the composite temperature and wind analyses at 500 and 700 mb., the isentropic flow pattern corresponds to a level not far from the base of the middle cloud. The implied vertical motion pattern should compare closely with that presented in figure 24. The greatest upward displacement of air isentropically occurs in the current of meridional flow which leads from south of 10° lat. into the shaded area. Conversely, sinking motion predominates almost everywhere west of the cloud shield. It may be presumed (see Carlson [1]) that the large-scale baroclinically induced vertical motion near the upper part of the trade-wind moist layer is primarily responsible for initiating a widespread convective and showery regime which provides a favorable environment for maintaining the intermittent development of a much deeper convection. The area in which this is thought to be occurring is represented by the stippling in figure 27 and corresponds to the stippled area, I, of figure 17.

One effect of the convection is the flux of water vapor from below and the redistribution of part of that moisture throughout the middle and upper troposphere through mixing of the convective updrafts with the environment. By this process the air at middle levels, which is normally

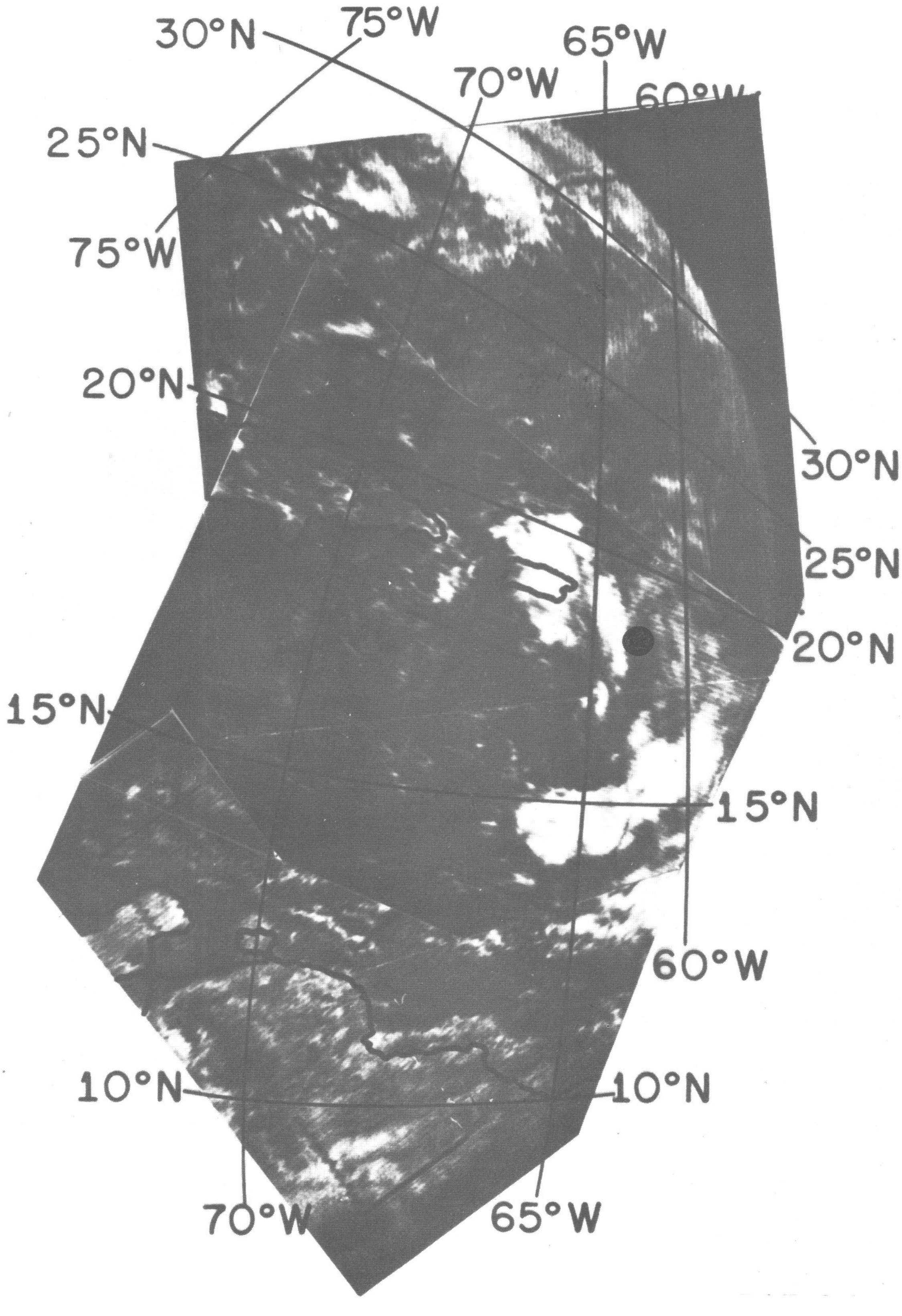

FIGURE 18.—TIROS X satellite photograph for 1537 GMT, October 17, 1965. The 250-mb. vortex center is indicated by a dot.

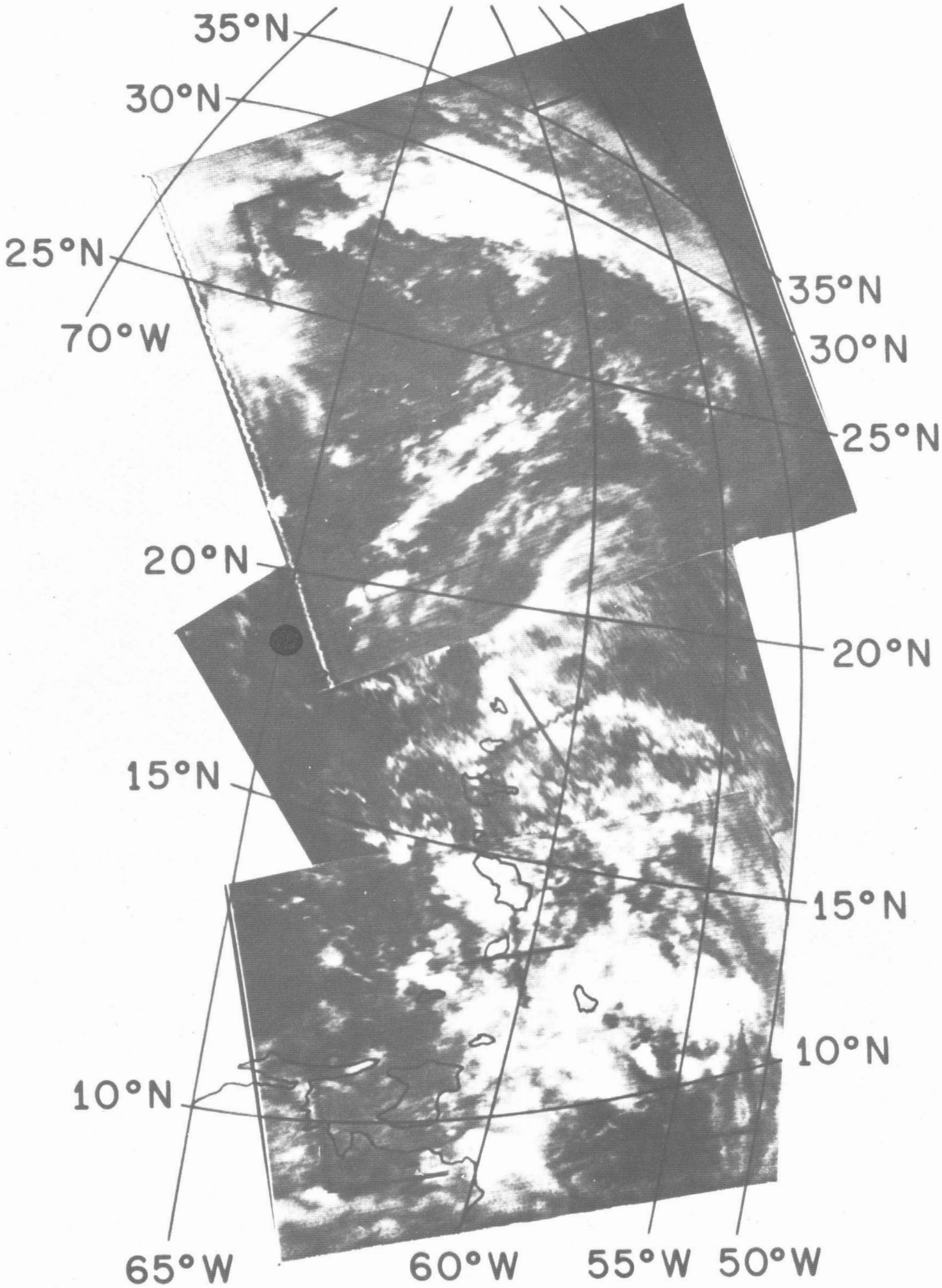

FIGURE 19.—TIROS X satellite photograph for 1551 GMT, October 18, 1965. The 250-mb. vortex center is indicated by a dot.

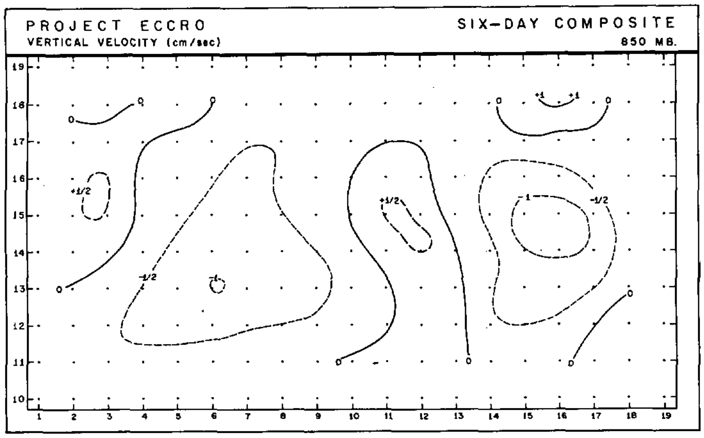

FIGURE 20.—Composited distribution of quasi-kinematic vertical velocity (cm./sec.) at 850 mb., October 12–18, 1965.

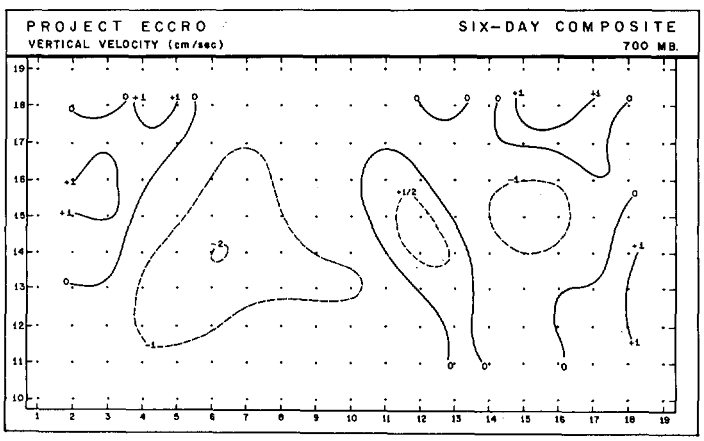

FIGURE 21.—Same as figure 20 but for 700 mb.

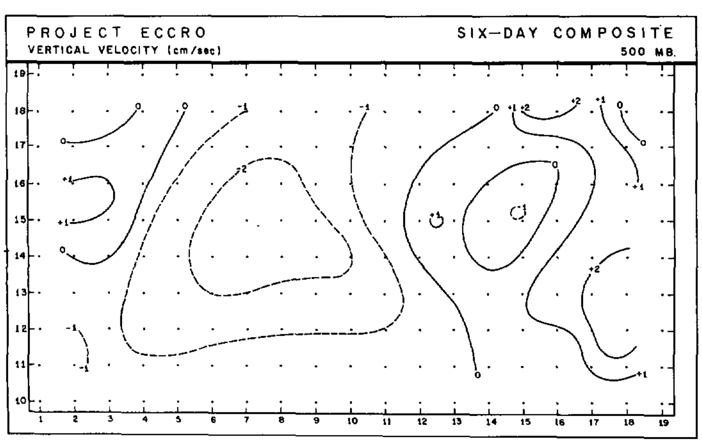

FIGURE 22.—Same as figure 20 but for 500 mb.

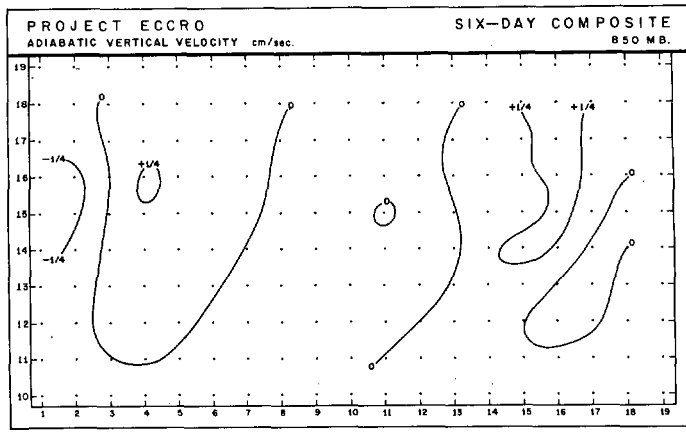

FIGURE 23.—Composited distribution of adiabatic vertical velocity (cm./sec.) at 850 mb., October 12–18, 1965.

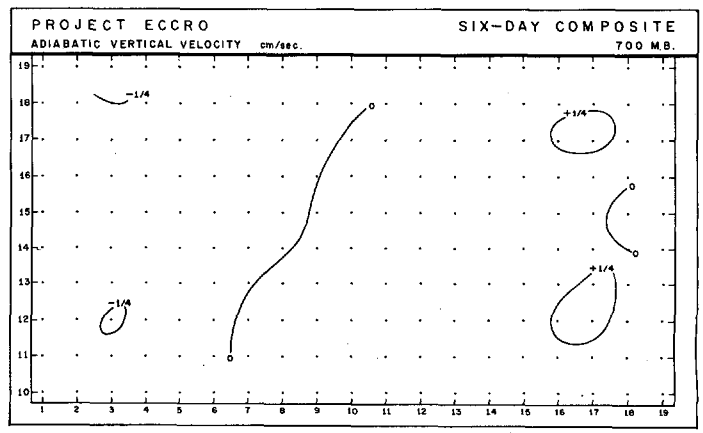

FIGURE 24.—Same as figure 23 but for 700 mb.

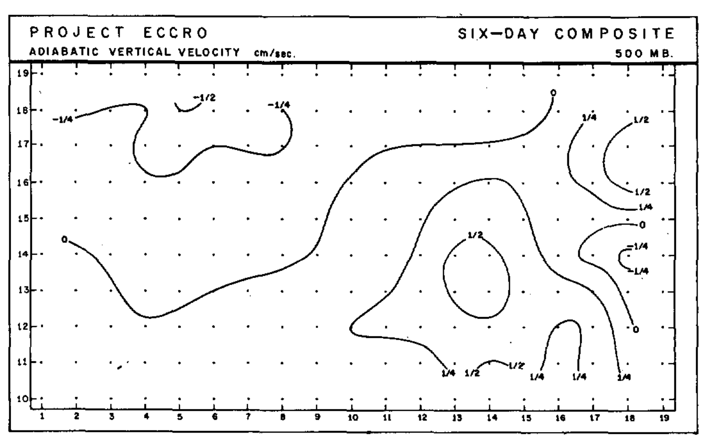

FIGURE 25.—Same as figure 23 but for 500 mb.

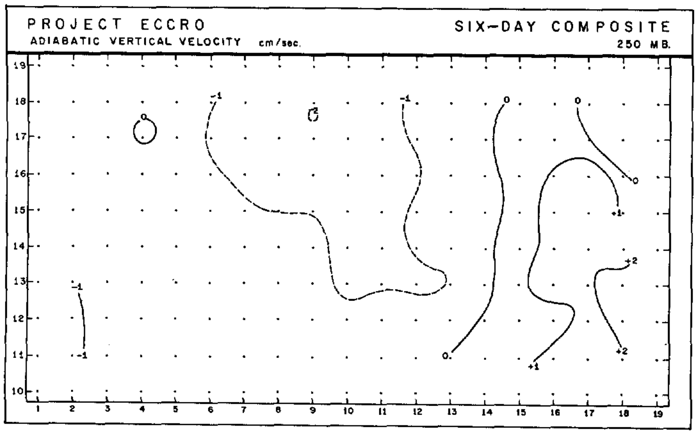

FIGURE 26.—Same as figure 23 but for 250 mb.

dry in the absence of organized convection, is brought quickly to saturation in the region of convection. Since the air moistened by convection is still subject to the dictates of the large-scale vertical motion pattern, which is shown to be existing simultaneously with the convection, its continued ascent forms a cloud shield in and downstream from the convective area.

Figure 28a presents a sounding made at Barbados whose relative position in the composite system, indicated by the symbol A in figure 27, lay in the immediate vicinity of the (stippled) convective area. The middle cloud is recognizable on the sounding as an almost saturated layer above 680 mb. In this layer the value of θ_w, the wet bulb potential temperature, was uniformly close to 20° C., or considerably higher than the 17.5° C. found

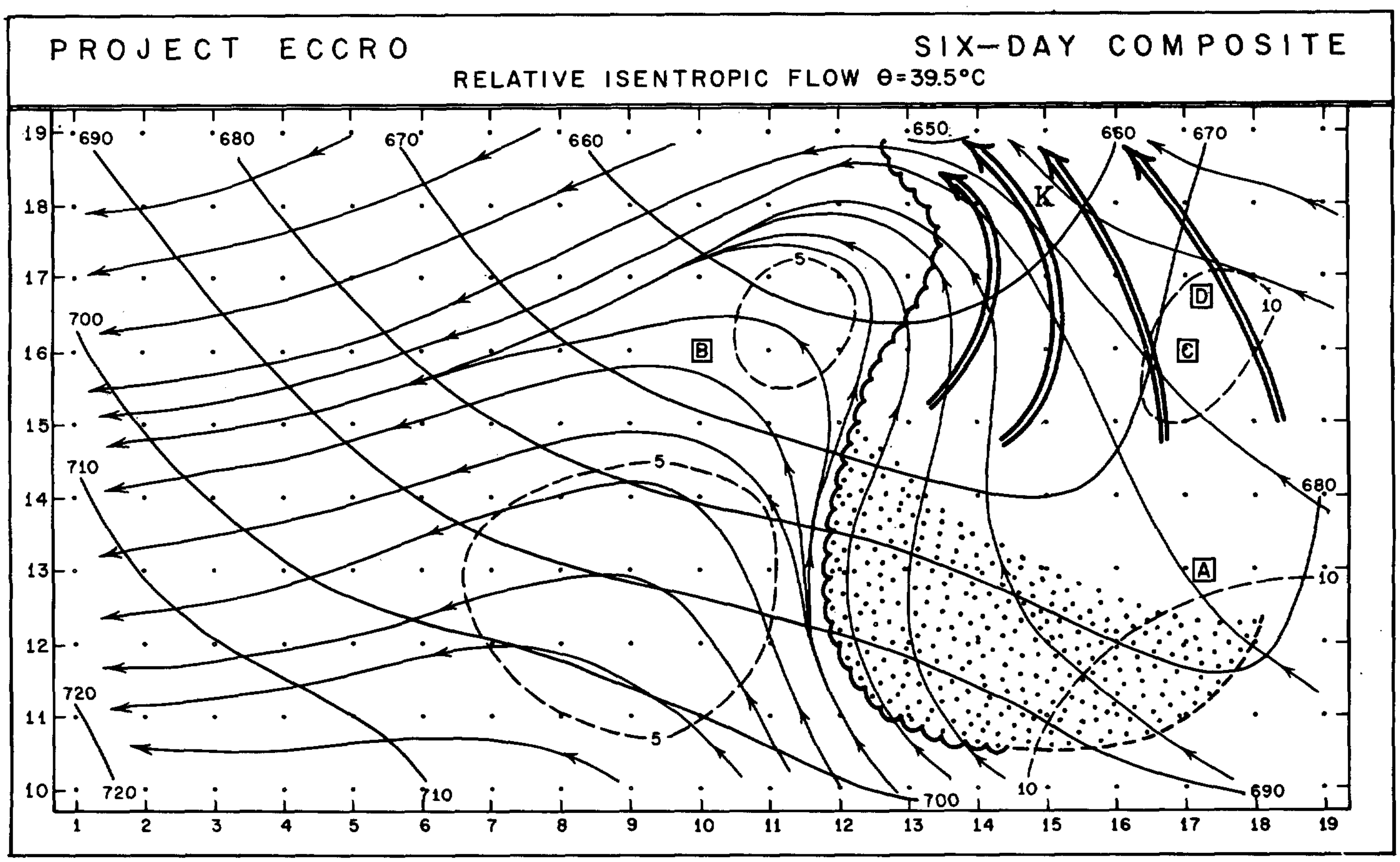

FIGURE 27.—Composited relative isentropic flow chart for the potential temperature surface, $\theta=39.5°$ C. Barbed (solid) lines represent streamlines and dashed lines are isotachs (in knots). Plain solid lines are pressure contours (in millibars) on isentropic surface. Shading denotes region of significant convection and corresponds to the shaded area of figure 17. Scalloped bordering delineates edge of main cloud shield. Heavy double arrows indicate direction of relative flow in the cloud layer and can be thought of as corresponding to the relative streamlines of wet isentropic motion, $\theta=20°$ C., which depart from those on the dry surface. The letters A, B, C, and D locate the four soundings referred to in figure 28 and K marks the center of the cold core.

on the Guadeloupe sounding in figure 28b (relative position B). The latter is situated in the descending current and exhibits the typically dry conditions aloft which are found on soundings in an undisturbed part of the subtropics not recently subjected to organized convection. As the cloudy air moved northward and ascended with the large-scale flow its base was found to become higher. On the soundings for Guadeloupe in figure 28c (relative position C) and Antigua in figure 28d (relative position D), which are located well to the north of the convective region, the cloud base is recognizable at 620 and 520 mb., respectively. The wet bulb potential temperature was also about 20° C. in the cloud layer at these stations. Figures 28c and 28d exhibit a segment of very dry air between the cloud base and 800 mb., the top of the moist layer. The value of θ_w in this dry segment is about 17.5° C., which, as previously stated, is characteristic of air at middle levels in an undisturbed region not recently affected by cumulus convection.

Although a substantial buoyancy is shown to exist in the lower levels of the soundings in figures 28c and 28d ($\theta_w \approx 22.5°$ C. over the bottom 100-mb. layer), very little rainfall occurred in the vicinity of these stations. While it seems quite likely that the amount and intensity of descending motion at lower levels east of the cold Low are highly exaggerated in the composite charts of quasi-kinematic vertical velocity (figs. 20–22), it is reasonable to believe that the suppressed convection and the dry layer found below the cloud base in the region north of the shaded area in figure 27 are associated with a general lack of ascent at low levels. Malkus and Riehl ([7], see p. 176) encountered a similar expanse of middle cloud and suppressed convection while flying through a disturbance in the Pacific. They showed that this cloud was originating in a distant bank of cumulonimbi upwind and their conclusion was that subsidence was occurring beneath the middle cloud in compensation for ascent in the region of significant convection.

Figures 28 a, c, and d show that the wind backed rapidly with height near the cloud base and that the easterly flow beneath the cloud was somewhat sharply differentiated from the more southerly flow above. It is presumed here that the motion of the cloudy air, which contained a θ_w of about 20° C., departed from the flow on the *dry* isentropic surface of figure 27 and began to move in a direction more accurately represented by the southerly flow above the isentropic surface; i.e., with the heavy double streamlines in figure 27. According to the TIROS satellite photographs, the western edge of the cloud shield remained east of the upper trough (but west of the center of cold air) north of lat. 19°N., the northern border of the analyzed area. Quite likely the flow within the cloud layer was turning from a southerly to a more westerly direction along the northern part of the cloud shield.

5. CONCLUDING REMARKS

As suggested by Frank [3] the distribution of cloudiness and vertical motion associated with a cold Low is not unlike that found in the vicinity of higher-latitude systems, such as troughs in the westerlies and occluded cyclones. On this occasion the cloud pattern lay in an extensive swath east of the upper trough and between lat. 10° and 25°N. Like its frontal counterpart at higher latitudes the cloud shield consisted primarily of ascending layers of altocumulus and cirrus, while the important convection was confined to a relatively small region far to the southeast of the vortex center near the lower end of the cloud shield.

The inferred trajectories in the cloud layer illustrate the meridional eddy transport of moisture through the system. Thus water vapor was being transported by the convection from the low-level easterlies south of lat. 15° N. and some of it redistributed to the atmosphere at middle and high levels, the remainder (and probably the bulk) of the moisture was falling out as rain. The moistening of the air aloft, in combination with the existing pattern of large-scale ascent, resulted in the formation of an extensive layer of middle and high cloud downstream. Accompanied by the release of latent heat and the further dispersal of moisture in scattered light showers, the cloudy air was conducted in the ascending current to still higher levels north of lat. 19°N. and thence into the westerlies.

In the view of the gradual weakening of the system, the energy processes for this cold Low probably were operating at least after the 14th, in the indirect sense. Further, it is reasonable to conclude that the considerable reduction in the amount and intensity of the convection on the 18th was brought about by the gradual weakening of the system and a decrease in its baroclinicity below some strength necessary to accommodate a sufficient lifting of the low-level air.

ACKNOWLEDGMENTS

The author greatly appreciates the various comments on the manuscript made by Mr. Harry Hawkins and Dr. Stanley Rosenthal of the National Hurricane Research Laboratory. Additional help was given by Mr. Robert Carrodus who was responsible for drafting the figures, Mr. Russell DeSouza who constructed the streamlines and isotachs for the individual maps, and Miss Debbie Nejman who did the typing.

REFERENCES

1. T. N. Carlson, "Isentropic Upslope Motion and an Instance of Heavy Rain Over Southern Florida," *Monthly Weather Review*, vol. **95**, No. 4, Apr. 1967, pp. 213–220.
2. T. N. Carlson, "Project ECCRO: A Synoptic Experiment in the Tropics," *ESSA Technical Memorandum*, IERTM-NHRL 80, Weather Bureau, National Hurricane Research Laboratory, Miami, Fla., Aug. 1967, 31 pp.

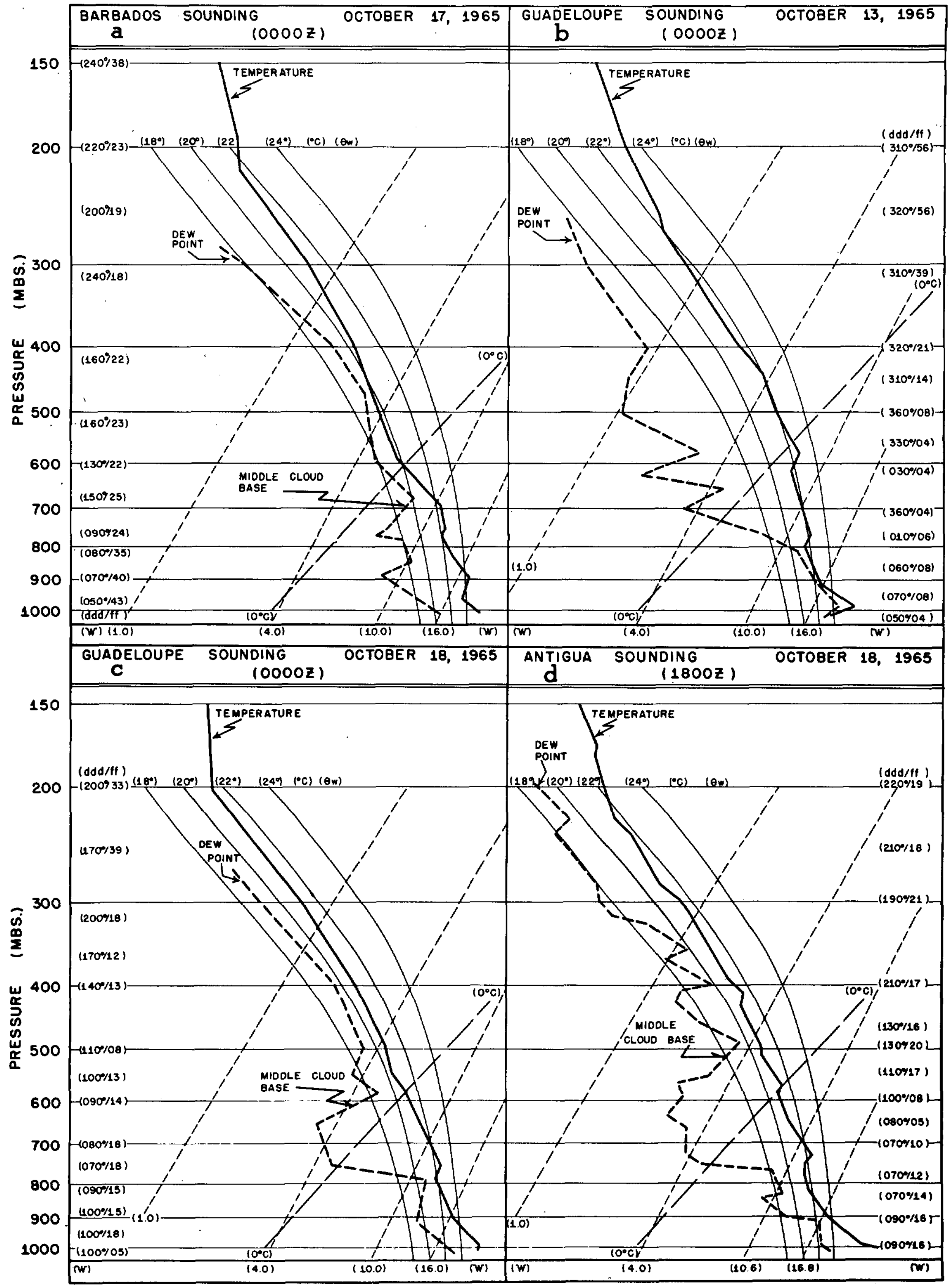

FIGURE 28.—Soundings located at relative positions A, B, C, and D in composite system (as indicated in figure 27): (a) at location A; (b) at location B; (c) at location C; and (d) at location D. Wet abiabats are labelled in ° C. The slanting dashed lines are for saturation mixing ratios and the heavy dashed line indicates the 0° C. isotherm. The vertical distribution of wind speed and direction (in degrees and knots) are entered at the side. The base of the middle cloud is indicated by an arrow.

3. N. L. Frank, "Synoptic Case Study of Tropical Cyclogenesis Utilizing Tiros Data," *Monthly Weather Review*, vol. 91, No. 8, Aug. 1963, pp. 355–366.
4. N. L. Frank, "The Weather Distribution With Upper Tropospheric Cold Lows in the Tropics," *Southern Region Technical Memorandum* No. 28, Weather Bureau, ESSA, National Hurricane Center, Miami, Fla., Sept. 1966, 22 pp.
5. T. N. Krishnamurti and D. Baumhefner, "Structure of a Tropical Disturbance Based on Solutions of a Multilevel Baroclinic Model," *Journal of Applied Meteorology*, vol. 5, No. 4, Aug. 1966, pp. 396–406.
6. M. A. Lateef, "A Case Study Concerning Vertical Motion, Divergence, and Vorticity in the Troposphere Over the Caribbean," *Monthly Weather Review*, vol. 95, No. 11, Nov. 1967, pp. 778–790.
7. J. S. Malkus and H. Riehl, *Cloud Structure and Distributions Over the Tropical Pacific Ocean*, University of California Press, Berkeley, 1964, 229 pp.
8. R. L. Ricks, "On the Structure and Maintenance of High Tropospheric Cold-Core Cyclones of the Tropics," M.S. Dissertation, Department of Meteorology, University of Chicago, 1959, 32 pp.
9. H. Riehl, *Tropical Meteorology*, McGraw-Hill Book Company, Inc., New York, 1954, 392 pp.
10. S. L. Rosenthal, "Some Theoretical Results Which Pertain to the Upper-Tropospheric Vortex Trains of the Tropics," *National Hurricane Research Project Report* No. 70, U.S. Weather Bureau, Apr. 1964, 27 pp.
11. R. H. Simpson, "Evolution of the Kona Storm, a Subtropical Cyclone," *Journal of Meteorology*, vol. 9, No. 1, Feb. 1952, pp. 24–35.

[Received June 26, 1967; revised August 21, 1967]